Simulation-Based Analysis of Train Controls under Various Track Alignments

Kitae Kim, M.ASCE[1]; and Steven I-Jy Chien, M.ASCE[2]

Abstract: This study develops a time-driven train performance simulation (TPS) model consisting of train traction module, track alignment module, and train control module, which is applied to emulate the movement of a train, calculate energy consumption, and estimate travel time, considering various vertical track alignments and operational controls. A numerical example is given in this study to demonstrate the features of the developed TPS, such as generating time varying operational measures (e.g., the tractive effort, resistance, acceleration rate, speed, and energy consumption, etc.) and calculating energy consumption and travel time. The most energy efficient train control, or called "golden run," associated with various track alignments, speed limits, and schedule adherence are identified, while the impact of coasting locations to travel time and energy consumption is also assessed. A sensitivity analysis is conducted, and the relationship between model parameters and control variables are discussed.

DOI: 10.1061/(ASCE)TE.1943-5436.0000160

CE Database subject headings: Rail transportation; Railroad tracks; Traffic assignment; Energy consumption; Simulation; Travel time.

Author keywords: Train control; Energy consumption; Simulation; Track alignment; Travel time.

Introduction

As a major public transportation mode, rail transit has been widely used in many metropolitan areas. Over the years, the consumed energy grows because of the increase of total line haul distance and passenger and train miles of travel. It was found that the annual energy usage increased 1.8 and 1.7% for passenger and freight rail services, respectively, from 1995 to 2006 [Energy Information Administration (EIA) 2007]. Solely in 2006, 584.5 trillion British thermal units (BTUs) and 101.1 trillion BTUs were, respectively, consumed by passenger and freight rail services. Due to the recent hike in gas and energy cost, significant number of travelers shifting from highway modes to transit is observed. This might drastically induce energy consumption and operating cost of rail transit systems.

According to the forecast of the U.S. Energy Information Administration, transportation energy consumption and energy price will continuously increase until 2030 [Energy Information Administration (EIA) 2007]. To alleviate expensive energy consumption bill and environmental impact, developing a model to evaluate and optimize train controls under various geometric and traffic conditions is desirable, which is the objective of this study.

In order to estimate energy consumption for various controls while operating a passenger train, considering track alignment, train schedule, and speed limits, a train performance simulation (TPS) model is developed. Various model outputs, including travel time and energy consumption in each motion regime can be generated, which can be applied to explore an optimal train control profile, or called "golden run," for minimum energy consumption operation subject to speed regulation and travel time constraints. A numerical example is given in this study to demonstrate the TPS features, such as generating time varying operational measures (e.g., the tractive effort, resistance, acceleration rate, speed, and energy consumption, etc.) and calculating energy consumption and travel time. The impact of coasting locations to travel time and energy consumption is also assessed, while evaluating the sensitivity of model parameters to energy consumption and travel time.

Literature Review

The U.S. Federal Railroad Administration initiated a study (1978) in developing TPS technology (e.g., in data collection, resistance modeling, power system modeling, brake system modeling, output data, and model validation, etc.) which triggered the railroad industry's attention on developing TPS models. The characteristics and features of TPS models that accommodate various predominant areas (e.g., fuel and energy usage, safety, and train operation studies) were evaluated by Howard et al. (1983). The sources of energy consumption in rail transit were classified into three categories: (1) train handling; (2) engineering modification; and (3) train makeup, in which data needed for TPS model design were identified.

Several models have been developed and applied to evaluate train controls and other research applications, including the assessment of rail signal system as well as the evaluation of timetables and interactions between trains meeting at complex junctions. Davis (1926) developed a train resistance equation con-

[1]Research Associate, Dept. of Civil and Environmental Engineering, New Jersey Institute of Technology, Newark, NJ 07102-1982 (corresponding author). E-mail: kk64@njit.edu

[2]Professor, Dept. of Civil and Environmental Engineering, New Jersey Institute of Technology, Newark, NJ 07102-1982. E-mail: chien@adm.njit.edu

Note. This manuscript was submitted on May 15, 2009; approved on April 12, 2010; published online on April 14, 2010. Discussion period open until April 1, 2011; separate discussions must be submitted for individual papers. This paper is part of the ***Journal of Transportation Engineering***, Vol. 136, No. 11, November 1, 2010. ©ASCE, ISSN 0733-947X/2010/11-937–948/$25.00.

sisting of rolling, journal, flange, and air resistances, based on the data of the Pennsylvania and Burlington Railroads. Later, a modified Davis equation [American Railway Engineering Association (AREA) 1981] was developed in 1970 by Committee 16 of American Railway Engineering Association, called AREA for adapting various train configurations, increased train operating speed, and improved track condition. Both equations were derived for calculating unit resistance while moving a train, in which weight per axle, number of axles per car, and vertical gradient; as well as the degree of aerodynamic and drag effects were considered.

In a study conducted by Hopkins (1975) and Hopkins et al. (1978), the energy consumption for various rail freight operation scenarios was measured based on train speed, car type, tractive effort, and car weight as well as track profile. It was found that the energy consumed by a train operated under a varying speed profile could cost 5 to 15% more than that under a constant speed profile. Note that the estimated energy consumption of both scenarios, which yielded the same average speed, was based on energy for propulsion only.

Hay (1982) discussed a number of kinetic equations for estimating the tractive effort, resistances, and gravitational acceleration rates. In addition, the effect of horizontal track alignments associated with allowable operating speeds for various degrees of curvatures and superelevations were also addressed. It was found that the resistances due to vertical gradient and horizontal curvature of track were 20 and 0.8 lb/t (1 lb=4.448 N, 1 t =907.2 kg) per track grade (in percentage) and per track curvature (in degree), respectively.

For simulating train controls and associated energy consumption, an energy management model developed by Uher and Disk (1987) consists of a train performance simulator and an electric network simulator. A method, which derived a forward and a backward speed profiles subject to the speed limits of a rail line, was applied for determining proper train speeds at any locations of the line so that the train can safely, accurately arrive at the next station. It was found that the intersection of the two speed profiles (e.g., backward and forward) is an initial point for braking.

Yasukawa et al. (1987) investigated various train controls for Tohoku Shinkansen electric motor trains in Japan. A simulation approach was employed to estimate energy consumption and travel time for various train controls, considering the motion regimes of cruising, coasting, and braking. Four different train controls, including (1) cruising and braking; (2) coasting, cruising, and braking; (3) cruising, coasting and braking; and (4) coasting, cruising, coasting and braking, were simulated on a rail segment between the stations of Ohmiya and Oyama. It was found that the fourth train control saved at least 10% of consumed energy compared to that with the rest of three controls.

Minciardi et al. (1994) applied a discrete, event based simulation approach to analyze the operation of a rail transit system. Two simulators, a stochastic event-driven simulator and an integrated system simulator, were employed to estimate energy consumption associated with the train movement. The simulation results were used for travel time and schedule adherence analysis. Since the simulation was purely based on discrete-event (e.g., train arrival to station, train departure from station, etc.), the kinematic impact to the train movement due to the geometry of track alignments was not considered.

Kim and Schonfeld (1997) developed a deterministic simulation model to analyze train performance on a convex rail alignment. The simulator computed propulsive and braking energy consumption based on tractive effort, resistance, the rate of acceleration/deceleration, and speed. A mathematical model was formulated to optimize dip percentage that significantly reduced energy consumption and travel time. The impact of dip percentage, station spacing, train power, and train controls were analyzed with and without speed constraints over the studied track alignment, but the coasting operation was not considered.

Chang et al. (1998) developed a simulation program, called interstation train movement simulation (ITMS), to evaluate automatic train operation. An object-oriented approach was employed to efficiently structure essential components, such as simulation clock, time driven objects (i.e., coasting time, braking time, etc.) and event driven objects (i.e., train door open, train departure from station, etc.). Several performance indicators, including speed, headway, and dwell time, under different signal control schemes for both steady state and stochastic conditions were analyzed. ITMS was applied to determine the optimal dwell time of the trains at stations in an effort to help ease passenger congestion conditions during peak period with fuzzy algorithms.

To test and improve advanced automatic train control (AATC), Gordon and Lehrer (1998) evaluated a train control simulator (TCS) developed by Bay Area Rapid Transit (BART) system in San Francisco. TCS consists of a train control and a train power simulator. The TCS was designed to handle the motion of a train traveling in both directions on a single track system and to predict the state of the power system at any given moment, while the train power simulator was designed to evaluate the severity of voltage sags and the usage of regenerated traction power. Through TCS, it was found that AATC enables more precise train control while coordinating operation involving multiple trains.

Jong and Chang (2005a,b) developed a train simulator, called TrainSim, using object-oriented programming concepts to generate speed profiles based on the shortest and normal operation times. The speed profiles recommended by TrainSim were compared to that generated by the Taiwan Railway Administration and has been demonstrated more efficient and flexible for train operation.

The American Railroad Engineering Association [American Railway Engineering Association (AREA) 1981] recommended railway design guidelines as well as construction and maintenance of railway infrastructure, which indicated that a vertical track profile will consists of segments with different grade percentages and transition sections, which needs sag and/or crest curves for smooth connection. Transition rates, denoted as γ, was estimated by Eq. (1), and the recommended transition rates are 0.05 and 0.1 for sag and crest curves, respectively

$$\gamma = \frac{(\delta_2 - \delta_1)}{l} \times 100 \tag{1}$$

where δ_1 and δ_2 are two adjacent track grades in percent and l =track length required for vertical curve in feet (ft).

Smith et al. (1990) examined the potential fuel savings of advanced railroad electronics system (ARES), the first positive train control system, for the Class I freight railroad [e.g., Burlington Northern Railroad (BNR) and Canadian National Railways (CNR)]. The ARES employed both an Energy Management System (EMS) to optimize train velocity profiles subject to schedule constraint, which minimizes fuel consumption. An algorithm that paces trains to arrive at specified locations and designated time was developed. Both BNR and CNR achieved a 2.5% fuel saving; equivalent to an annual saving of $79,775,000, after implementing the pacing algorithm and more efficient dispatching.

Numerous studies were found in developing TPS for estimat-

J. Transp. Eng. 2010.136:937-948.

ing energy consumption and travel time, while most of them were focusing on analyzing the effects of varying train speed with different motion regimes (e.g., acceleration, coasting, cruising, and deceleration). Little effort was found on simulating the joint effect of track alignment, train schedule, and train controls on energy consumption, which is focused in this study.

The proposed TPS model discussed in this paper employs the kinematic laws of motion in estimating energy consumption and travel time considering track alignment, train control, and train schedule, while commercial off-the-shelf train simulators use average run times in computing the train movement (Julich et al. 1999). The equations and logic used in the three modules [i.e., train traction module (TTM), track alignment module (TAM), and train control module (TCM)] of the TPS are justifiable based on operation condition (e.g., station spacing, applied motion regime, and scheduling, etc.), operating safety regime (e.g., normal, emergency, and instant braking), track profile, and locomotive characteristics (e.g., horsepower, train weight, maximum and minimum speeds, etc.). In addition, the accuracy of the proposed TPS can be enhanced by calibrating train performance parameters such as transmission efficiency, acceleration/deceleration rates, and braking efficiency.

Model Development

A time-driven TPS model is developed here consisting of three key modules: TTM, TAM, and TCM, which is designed to evaluate travel time and energy consumption for various train controls and track alignments. Time dependent information, such as the tractive effort, resistances, the rate of acceleration/deceleration, and speed, are generated corresponding to the location of a train and the geometry of the track alignment. The development of each module is discussed below.

Train Traction Module

The responsibility of the TTM is to compute the required tractive force to move a train along a rail line, considering the prevailing speed, the rates of acceleration and deceleration, and the location of the train at any time point. TTM calculates the tractive effort based on projected resistances so that the rates of acceleration/deceleration and the target speed for next interval operation can be calculated. The input parameters of TTM include static information (e.g., locomotive power, number of cars per train, number of axles per car, train weight, and cross section area, etc.), dynamic information (e.g., train location, travel time, speed, rates of acceleration/deceleration), track alignment condition (e.g., level, convex, concave, etc.), and operational constraints (e.g., speed limit, station spacing, and train schedule, etc.). An iterative computation process is performed based on user-specified time interval (e.g., 1 s), in which the needed tractive effort which move the train to the desired location over time can be determined.

The calculated tractive effort with TTM can be applied to different types of locomotives (e.g., diesel-electric and electric motors) for estimating consumed energy by justifying the ratio of energy consumption per unit of the tractive effort. Note that the function of the tractive effort is calculated based on the effective power to move tonnage up on the track alignment (e.g., level, convex, and concave).

In order to avoid slippage of the wheel on the track, the maximum tractive effort at time t, denoted as $F^t_{\max}$, is the minimum value of available propulsive force, denoted as F^t_p, and adhesive force, denoted as F^t_a. Thus

$$F^t_{\max} = \min(F^t_p, F^t_a) \quad \forall\, t \tag{2}$$

where F^t_p, the needed force to overcome the resistance, is the product of locomotive's horse power, denoted as P^t, and transmission efficiency, denoted as η, divided by speed in miles per hour (mi/h, 1 mi/h=1.609 km/h), denoted as V^t, at time t. Thus

$$F^t_P = \frac{375 \cdot \eta \cdot P^t}{V^t} \quad \forall\, t \tag{3}$$

where 375=parameter to convert the unit rate of work in foot-pounds (1 ft=0.3048 m, 1 lb=0.4535 kg)/second into mile-pounds/hour (Hay 1982). Note that η, varying with the type of gears, is usually between 0.78 and 0.85 depending on train speed and track condition.

On the other hand, F^t_a, a friction force caused by the contact between the wheel and the track surfaces, is affected by the train weight, denoted as W, and adhesive coefficient, denoted as μ^t. The determination of μ^t is based on the train speed as shown in Fig. 1 (Vuchic 2007), which ranges between 0.28 and 0.38 for a train speed of 10 km/h and decreases as the speed increases. In this study, μ^t is assumed linearly decreasing as the speed decreases from 0 to 80 km/h and derived as

$$\mu^t = 0.33 - 0.002 \cdot V^t \quad \forall\, t \tag{4}$$

The kinematics of a train movement at time t inclined at an angle θ^t to the horizontal are determined by the tractive effort, resistances and the train weight, denoted as F^t_{TE}, R^t, and W, respectively (see Fig. 2). The adhesive force (F^t_a) for steel wheels on the rail, caused by train weight perpendicular to the surface of the track, can be estimated by Eq. (5) as

$$F^t_a = \mu^t W \cos\theta^t \quad \forall\, t \tag{5}$$

where θ^t=track gradient in degrees.

The train resistances considered in TPS include bearing resistance, rolling resistance, and aerodynamic resistance. The first two resistances purely depend upon the speed and weight of the train, while the third one is affected by the direction and speed of

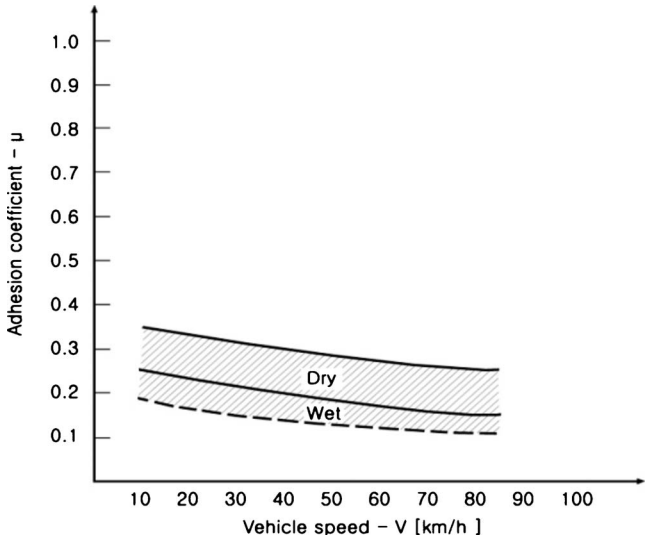

Fig. 1. Adhesion coefficient versus speed under different rail and wheel conditions

J. Transp. Eng. 2010.136:937-948.

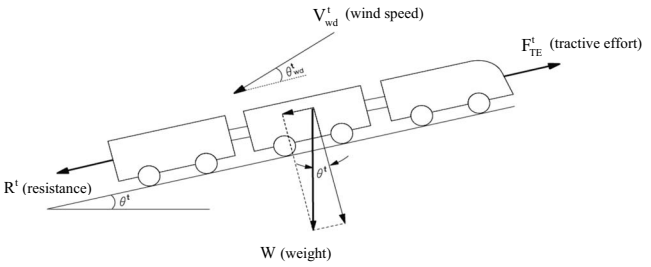

Fig. 2. Tractive effort and resistance diagram on a track with inclination

wind as well as the size, shape, and speed of the train. The unit train resistance at time t, denoted as r^t in unit of lb/ton (1 lb =4.448 N, 1 t=907.2 kg), can be obtained by employing the modified Davis Equation (Hay 1982) as

$$r^t = 0.6 + \frac{20}{w} + 0.01 \cdot V^t + \frac{K \cdot (V^t_R)^2}{w \cdot n} + 20 \cdot G^t + 0.8 \cdot D^t \quad \forall\, t \tag{6}$$

where w represents car weight per axle; G^t represents grade percentage; D^t represents track curvature; and K and n =aerodynamic coefficient and the number of axles per car, respectively. Note that V^t_R represents relative train speed based on the direction of wind speed (V^t_{wd}) as shown in Fig. 2. Thus, $V^t_R = V^t + \cos\theta^t_{wd} \cdot V^t_{wd}$ where θ^t_{wd}=angle between the directions of wind and the train movement.

The total train resistance at time t, denoted as R^t, is the product of unit resistance (r^t), car weight per axle (w), number of axles per car (n), and number of cars per train (N_{TR}). Thus

$$R^t = r^t \cdot w \cdot n \cdot N_{TR} \quad \forall\, t \tag{7}$$

Therefore, the net force to move a train is equal to the tractive effort minus the resistance, which is equivalent to the product of acceleration rate, denoted as a^t, and the mass of the train, denoted as m. Thus

$$F^t_{TE} - R^t = a^t \cdot m \quad \forall\, t \tag{8}$$

Note that the net force at time t divided by the train mass represents acceleration, denoted as a^t. Thus

$$a^t = \frac{(F^t_{TE} - R^t) \cdot g}{\rho \cdot W} \quad \forall\, t \tag{9}$$

where ρ and g=coefficients of rotating mass and gravitational acceleration, respectively.

The process of calculating train deceleration is similar to that for calculating acceleration, which is determined by actual braking force, denoted as F^t_b, the maximum value of comfort-limited braking force, denoted as F_{bc}, and adhesion-limited braking force, denoted as F_{ba}. Thus

$$F^t_{B(\max)} = \max(F^t_{bc}, F^t_{ba}) \quad \forall\, t \tag{10}$$

By considering the comfort of standees, F_{bc} is regulated not to exceed the maximum deceleration rate, denoted as b_{max}. According to Eq. (8), Eq. (11) can be derived for F_{bc}, in which the maximum rate of acceleration is replaced by the maximum rate of deceleration. Thus

$$F^t_{bc} = b_{\max} \cdot \left(\frac{W}{g}\right) \cdot \rho + R^t \quad \forall\, t \tag{11}$$

Unlike F_{bc}, F_{ba} is caused by adhesion between the track and the wheel while braking, which has been discussed in Eq. (5).

The train acceleration rate shall not exceed the maximum acceleration rate, denoted as a_{max}, for both safety and passenger comfort concerns. In this regard, the suggested maximum acceleration and deceleration rates are formulated as Eqs. (12) and (13), respectively (Hoberock 1977)

$$a_{\max} \le 0.15 \cdot g \tag{12}$$

$$b_{\max} \ge -0.15 \cdot g \tag{13}$$

Since the train tractive force in the proposed TPS model is calculated based on user specified time interval, denoted as Δt, the train speed and the distance of travel within Δt can be estimated based on the rate of acceleration or deceleration. The speed difference, denoted as ΔV^t, from t to $t+1$ is the product of acceleration rate and Δt as formulated in Eq. (14), and the travel distance, denoted as Δx^t, is the average speed between time t and $t+1$ multiplied by Δt as formulated in Eq. (15)

$$V^{t+1} = V^t + \Delta V^t = V^t + a^t \cdot \Delta t \quad \forall\, t \tag{14}$$

$$x^{t+1} = x^t + \Delta x^t = x^t + \left(\frac{v^t + v^{t+1}}{2}\right) \cdot \Delta t \quad \forall\, t \tag{15}$$

To move a train with speed V^t, Eq. (16) recommended to calculate the engine power consumed at t, called P^t, is applied (Hay 1982)

$$P^t = \frac{F^t_{TE} \cdot V^t}{375 \cdot \eta} \quad \forall\, t \tag{16}$$

Thus, the energy consumption rate, denoted as e^t, for either propelling or braking during Δt is derived as

$$e^t = P^t \cdot \Delta t \cdot 0.7457 \cdot \frac{1}{3{,}600} = P^t \cdot \Delta t \cdot 0.000\,207 \quad \forall\, t \tag{17}$$

Note that the unit engine power (hp) is equal to 0.7457 kW (kW), and the interval time (s) divided by 3,600 is converted to an hourly base. The total energy consumption, denoted as E, over the route segment can be obtained by integrating the required power over time. Thus

$$E = \sum_{t=1}^{J} \Delta e^t \quad \forall\, t \tag{18}$$

where J=number of time intervals needed for traveling from one station to another.

Track Alignment Module

TAM converts a given vertical track profile into a series of track grades delivered to TTM for calculating train resistances and the needed tractive effort, which exchanges data (e.g., track grade and train position) in every simulation time step. TAM also provides information (e.g., maximum operating speed, denoted as V_M, and civil speed restriction) to the Train Control Module (TCM) so that a proper track alignment can be referred to determine the regime of motion (e.g., acceleration, cruising, coasting, and deceleration, etc.). A step procedure summarized below discusses the interaction between TAM and other modules (e.g., TTM and TCM).

J. Transp. Eng. 2010.136:937-948.

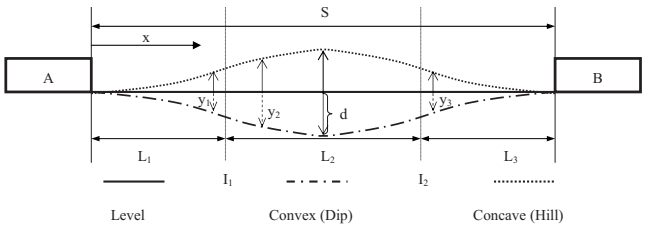

Fig. 3. Vertical track alignment between Stations A and B

- Step 1: identify the number of inflection points of a track alignment between a pair of stations which divide the station spacing (S) into a number of segments with length of L_i for segment i

$$S = \sum_{i=1}^{q} L_i \tag{19}$$

where q=number of segment.

- Step 2: develop equations y_i^t for all segment i, which represent vertical track alignments for all segments in Step 1. y_i^t varies with the traveled distance at time t (x^t).
- Step 3: differentiate y_i^t over distance to obtain track grade, denoted as G_i^t, for segment i

$$G_i^t = \frac{\partial y_i^t}{\partial x^t} \quad \forall\, t \tag{20}$$

- Step 4: input G^t to TTM and y_i^t to TCM to calculate the resistances and the tractive effort and determine the regime of motion at t.
- Step 5: input G^t and V_M to TTM every time interval and receive travel distance (Δx^t) data from TTM, where $\Delta x^t = x^t - x^{t-1}$. Note that V_M on a designated track segment is the speed limit, which is known prior to commencing the TPS.

As shown in Fig. 3, for example, the divided segments from a vertical alignment (e.g., symmetric and parabolic) can be categorized into three types of curves: level, convex, and concave. In order to obtain continuous vertical track profile and track gradient, a general track alignment must be formulated, considering the station spacing (S), locations of inflection points (I_1 and I_2), vertical height/depth (d) at halfway between Stations A and B.

Train Control Module

The mission of the TCM is to determine appropriate motion regime based on the tractive effort and the track alignment information computed by TTM and TAM. TCM then first generate feasible control plans formed by different motion regimes. As shown in Fig. 4, a general train control, denoted as TC, consisting of accelerating (M_a), first coasting (M_{c_1}), cruising (M_v), second coasting (M_{c_2}), and braking (M_b), is developed for discussing feasible plans. Note that the relationship between speed and time is not necessarily a linear function and some motion regimes may be excluded by setting the associated times equal to 0.

While M_a and M_b are always essential for accelerating and decelerating a train departing from and arriving at a station, three other motion regimes (e.g., M_{c_1}, M_v, and M_{c_2}) are optional and can be flexibly included to work with M_a and M_b. For instance, if the durations for the 1st and 2nd coasting regimes are equal to zero (e.g., $t_{c_1}=t_{c_2}=0$), the resulting train control only consists of accelerating, cruising, and braking regimes. However, if the durations for the 1st coasting and cruising are equal to zero (e.g., $t_{c_1}=t_v=0$), the resulting train control consists of the regimes of accelerating, coasting, and braking. It is well recognized that coasting is usually a beneficial motion regime in terms of energy saving; however longer travel time should be expected. Therefore, a challenging research problem is where and when the coasting regime should be applied, subject to speed and travel time constraints.

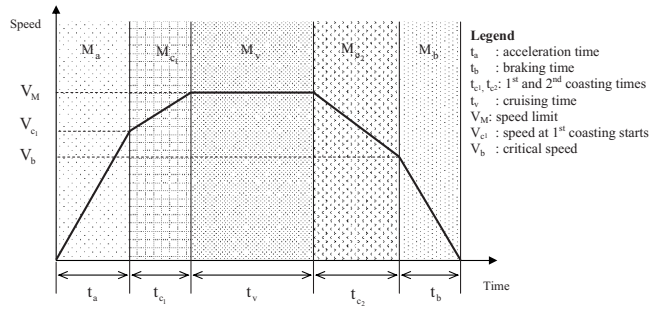

Fig. 4. Configuration of a speed profile for general train control

Considering different controls (e.g., combinations of applicable motion regimes) on various track alignments (e.g., level, convex, and concave), the feasible train controls for each type of alignments are summarized in Table 1. Note that for the 1st, 2nd, and 3rd train control on a level track alignment are denoted as TC_1^{LV}, TC_2^{LV}, and TC_3^{LV}, respectively.

- $\mathrm{TC}_1^{\mathrm{LV}}$: considering cruising regime (M_v) associated with M_a and M_b;
- TC_2^{LV}: considering cruising and both coasting regimes (e.g., M_{c_1} and/or M_{c_2}) associated with M_a and M_b; and
- TC_3^{LV}: considering coasting regimes (e.g., M_{c_1} and/or M_{c_2}) associated with M_a and M_b.

While a general train control consists of five motion regimes, M_a, M_{c_1}, M_v, M_{c_2}, and M_b, the station-to-station travel time denoted as T (excluding dwell time at stations) can be formulated as

$$T = t_a + t_{c_1} + t_v + t_{c_2} + t_b \tag{21}$$

where t_a, t_{c_1}, t_v, t_{c_2}, and t_b represent travel times (sec) for acceleration, 1st coasting, cruising, 2nd coasting, and braking, respectively, which can be calculated with Eqs. (22*a*)–(22*e*) formulated as

$$t_a = \frac{1.47 \cdot V_{c_1}}{\bar{a}} \tag{22a}$$

Table 1. Feasible Train Controls and Motion Regimes

Track alignment		Train controls and motion regimes
Level	(1)	$\mathrm{TC}_1^{\mathrm{LV}} = M_a + M_v + M_b$
	(2)	$\mathrm{TC}_2^{\mathrm{LV}} = M_a + M_v + M_{c_2} + M_b$
	(3)	$\mathrm{TC}_3^{\mathrm{LV}} = M_a + M_{c_2} + M_b$
Convex	(1)	$\mathrm{TC}_1^{\mathrm{CX}} = M_a + M_v + M_b$
	(2)	$\mathrm{TC}_2^{\mathrm{CX}} = M_a + M_{c_1} + M_v + M_{c_2} + M_b$
	(3)	$\mathrm{TC}_3^{\mathrm{CX}} = M_a + M_{c_1} + M_{c_2} + M_b$
Concave	(1)	$\mathrm{TC}_1^{\mathrm{CV}} = M_a + M_v + M_b$
	(2)	$\mathrm{TC}_2^{\mathrm{CV}} = M_a + M_{c_1} + M_v + M_b$
	(3)	$\mathrm{TC}_3^{\mathrm{CV}} = M_a + M_{c_1} + M_b$

J. Transp. Eng. 2010.136:937-948.

$$t_{c_1} = \frac{1.47(V_M - V_{c_1})}{\overline{c_1}} \tag{22b}$$

$$t_v = \frac{S_v}{1.47 \cdot V_M} \tag{22c}$$

$$t_{c_2} = \frac{1.47(V_M - V_b)}{\overline{c_2}} \tag{22d}$$

$$t_b = \frac{1.47 \cdot V_b}{\overline{b}} \tag{22e}$$

where 1.47=parameter to convert the speed in mph into feet per second (ft/sec, 1 ft=0.3048 m). Note that $\overline{a}$, $\overline{c_1}$, $\overline{c_2}$, and $\overline{b}$ represent the average rates of acceleration, 1st coasting acceleration, 2nd coasting deceleration, and deceleration, while V_{c_1} and V_b are the speeds where the 1st coasting begins and the critical speed where the maximum deceleration must apply. In Eq. (22*c*), S_v represents the distance consumed for vehicle cruising. Thus, the station-to-station travel time can be derived as

$$T = \frac{1.47 \cdot V_{c_1}}{\overline{a}} + \frac{1.47(V_M - V_{c_1})}{\overline{c_1}} + \frac{S_v}{1.47 \cdot V_M} + \frac{1.47(V_M - V_b)}{\overline{c_2}} + \frac{1.47 \cdot V_b}{\overline{b}} \tag{23}$$

As the travel time consumed by each motion regime is known, the station spacing (S) is equal to the sum of the distances travel with the applied motion regimes. Thus

$$S_a = \frac{1}{2}\overline{a}t_a^2 \tag{24a}$$

$$S_{c_1} = \frac{1.47}{2}(V_M + V_{c_1})t_{c_1} \tag{24b}$$

$$S_v = 1.47 \cdot V_M \cdot t_v \tag{24c}$$

$$S_{c_2} = \frac{1.47}{2}(V_M + V_{c_2})t_{c_2} \tag{24d}$$

$$S_b = \frac{1}{2}\overline{b}t_b^2 \tag{24e}$$

where S_a, S_{c_1}, S_{c_2}, and S_b represent the travel distances for acceleration, the 1st coasting, the 2nd coasting, and deceleration, respectively. Thus, the station spacing denoted as S can be formulated as

$$S = 1.47\left(\frac{V_{c_1}^2}{2\overline{a}} + \frac{V_M^2 - V_{c_1}^2}{2\overline{c_1}} + V_M \cdot t_v + \frac{V_M^2 - V_b^2}{2\overline{c_2}} + \frac{V_b^2}{2\overline{b}}\right) \tag{25}$$

The cruising time (t_v) is equal to the difference between the station spacing and the distance traveled during the regimes of acceleration, 1st coasting, 2nd coasting, deceleration divided by V_M. Thus

$$t_v = \frac{S - (S_a + S_{c_1} + S_{c_2} + S_b)}{1.47 \cdot V_M} \tag{26}$$

With Eqs. (25) and (26), the cruising time can be derived as

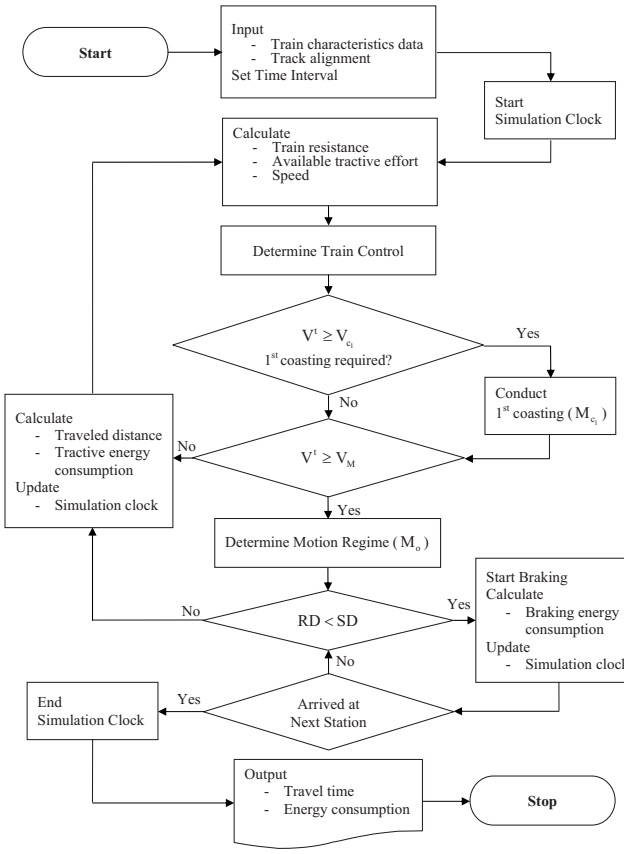

Fig. 5. Flowchart of the proposed TPS model

$$t_v = \frac{S}{1.47 \cdot V_M} - \frac{1.47 \cdot V_M}{2}\left(\frac{1}{\overline{c_1}} + \frac{1}{\overline{c_2}}\right) - \frac{1.47 \cdot V_{c_1}^2}{2V_M}\left(\frac{1}{\overline{a}} - \frac{1}{\overline{c_1}}\right) - \frac{1.47 \cdot V_b^2}{2V_M}\left(\frac{1}{\overline{b}} - \frac{1}{\overline{c_2}}\right) \tag{27}$$

The developed TPS model can simulate train movement every second on an iterative basis. A complete cycle of the proposed TPS calculation in each time interval is shown in Fig. 5, and the step procedure is discussed below.

- Step 1. Start the simulation and feed input data (e.g., motor power, car weight per axle, number of car, number off axle, etc.) to TTM and TAM.
- Step 2. Calculate the tractive effort, resistances, and speed at time t with TTM.
- Step 3. Determine the suitable train control. If the 1st coasting (M_{c_1}) can be applied at time t (e.g., $V^t \geq V_{c_1}$) with TCM, the 1st coasting begins. Otherwise, go to Step 4.
- Step 4. If $V^t \geq V_M$ with TTM, go to Step 6. Otherwise, calculate traveled distance and consumed energy for acceleration, update simulation clock (e.g., set $t=t+1$), and go to Step 2.
- Step 5. Determine the motion regimes (e.g., M_v, M_{c_2}, and $M_v+M_{c_2}$) with TCM.
- Step 6. If the remaining distance (RD) is less than the stopping distance (SD), the motion regime of deceleration begins. Calculate consumed braking energy in TTM, update the simulation clock, and go to Step 7. Otherwise, go to Step 2.
- Step 7. If the train arrives at a station, end simulation clock, report consumed travel time and energy, and terminate the simulation. Otherwise, go to Step 6.

J. Transp. Eng. 2010.136:937-948.

Table 2. Input Parameters of the Proposed TPS

Variables	Values
Station spacing (S)	3,600 m (12,000 ft)
Vertical dip/height (d)	27.4 m (90 ft)
Dip/height percentage ($d/S\times 100$)	0.75%
Motor power	2,237 kWh
Number of cars per train	6 cars/train
Car weight	36,288 kg/car (80,000 lb/car)
Maximum acceleration rate	1.47 m/s^2 (4.83 ft/s^2)
Maximum deceleration rate	−1.47 m/s^2 (−4.83 ft/s^2)
Air drag coefficient	0.007
Ruling grade	3%
Cross section area	10.5 m^2 (113 ft^2)
1st coasting (speed)	89, 97[a] km/h (≅55, 60 [a] mi/h)
2nd coasting (position from Station A)	1,828 m (6,000 ft)
Maximum operating speed (V_M)	105 km/h (65 mi/h)
Simulation time interval	0.5 s
Wind speed (V^t_{wd})	0 km/h

[a]For concave segment only.

Numerical Example

The purpose of this section is to demonstrate the applicability of the developed simulation model on estimating station-to-station travel time and energy consumption under various train controls and track alignments. A 6-car passenger train is considered whose motor power is 3,000 hp (=2,237 kWh). The maximum operating speed (V_M) is 105 km/h (=65 mi/h), and the acceleration rate is determined by the tractive effort, which will not exceed $0.15g$ (=1.47 m/s^2=4.83 ft/s^2) concerning passenger comfort. Also, a maximum train deceleration rate, $-0.15g$ (=−1.47 m/s^2= −4.83 ft/s^2) is applied. Other input parameters employed for the baseline simulation are summarized in Table 2.

The vertical profile is divided into three parabolic track alignments, as shown in Fig. 3, of which the equation for vertical segment i is formulated in Eq. (28) as

$$y_i^t = \begin{cases} -\dfrac{12d}{S^2}(x^t)^2, & i=1, \quad 0 \le x^t \le \dfrac{S}{6} \\ \dfrac{6d}{S^2}(x^t)^2 - \dfrac{6d}{S}x^t + \dfrac{d}{2}, & i=2, \quad \dfrac{S}{6} \le x^t \le \dfrac{5S}{6} \\ -\dfrac{12d}{S^2}(x^t)^2 + \dfrac{24d}{S}x^t - 12d, & i=3, \quad \dfrac{5S}{6} \le x^t \le S \end{cases} \tag{28}$$

where y_i^t represents elevation with respect to x^t in feet on segment i with length of 1/6, 2/3, and 1/6 of S for $i=1$, 2, and 3, respectively. Note that if $d=0$, the vertical track profile is level. For $d<0$ and $d>0$, the concave and convex vertical profiles are applied, respectively.

By differentiating Eq. (28), continuous track gradient for each segment can be achieved as

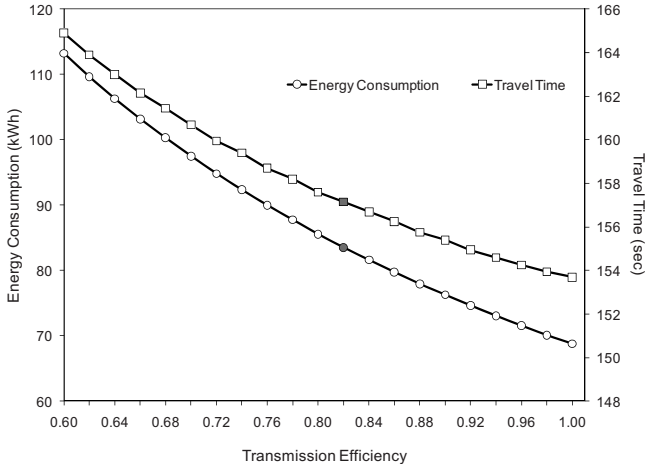

Fig. 6. Transmission efficiency versus energy consumption and travel time

$$G_i^t = \begin{cases} -\dfrac{24d}{S^2}x^t, & i=1, \quad 0 \le x^t \le \dfrac{S}{6} \\ \dfrac{12d}{S^2}x^t - \dfrac{6d}{S}, & i=2, \quad \dfrac{S}{6} \le x^t \le \dfrac{5S}{6} \\ -\dfrac{24d}{S^2}x^t + \dfrac{24d}{S}, & i=3, \quad \dfrac{5S}{6} \le x^t \le S \end{cases} \tag{29}$$

where G_i^t=gradient at x^t in percent.

For every simulation model, validation is essential to be conducted such that the desired level of confidence in the results of a simulation may be expected. The proposed TPS employs kinematic equations for estimating resistance, acceleration (or deceleration), and energy consumption, which are well known and validated by a locomotive of any horsepower in the previous studies (Hay 1982).

Note that the consumed energy is computed by the tractive effort, speed, and transmission efficiency (η) for train movement at time t. Since η significantly affects energy consumption and travel time, a suitable value must be found to produce accurate result. It was found that from Fig. 6 both energy consumption and travel time decrease as η increases. Note that the transmission efficiency value applied in the TPS is 0.82, which was confirmed by both electric and diesel-electric trains in the previous studies (Jong and Chang 2005a,b; Hay 1982).

Results of consumed energy and travel time from the developed TPS and the model developed by a previous model were compared under the same inputs to simulations (e.g., station spacing, track alignment, tractive effort, train control, etc.) In general, both models produce consistent output. For example, the consumed energy decreases and travel time increases as the dip percentage increases. It was found that the consumed energy estimated by the developed TPS is greater than that by the previous model under level and convex track alignments, but longer travel time was observed for a train to finish its journey. The difference was incurred by using different train resistance equations and μ^t, which affect the calculation of acceleration rate and adhesive force, and location where the brake began. Note that the energy consumption and travel time were not evaluated by the previous model as shown in Table 3.

J. Transp. Eng. 2010.136:937-948.

Table 3. Comparison of Simulation Results

		Level		Convex (0.5%)		Convex (1.0%)		Concave (0.5%)		Concave (1.0%)	
		(1)	(2)	(1)	(2)	(1)	(2)	(1)	(2)	(1)	(2)
Energy (kWh)	Tractive	75.6	65.8	71.9	61.4	68.5	58.4	—	68.9	—	73.9
	Braking	58.5	49.2	53.6	45.7	49.3	42.1	—	54.9	—	60.8
Travel time (s)		119	130.5	114.7	124.7	113.5	119.8	—	137.4	—	146.1

Note: (1)=model by Kim and Schonfeld (1997); (2)=developed TPSs.

Estimation of Travel Time

In order to understand the impact of track alignments, train controls, and maximum operating speed (i.e., 105 km/h) to the relationship of speed versus travel time, Figs. 7(a–c) were developed. For a level (flat) alignment as shown in Fig. 7(a), the relationship between speed and travel time was affected by where the coasting regime started. It was found that the travel time increases as coasting started earlier.

For a convex alignment as shown in Fig. 7(b), the maximum operating speed can be achieved by taking the advantage of down-hill alignment with coasting. The speed versus travel time diagram is therefore different from Fig. 7(a). It was found that the

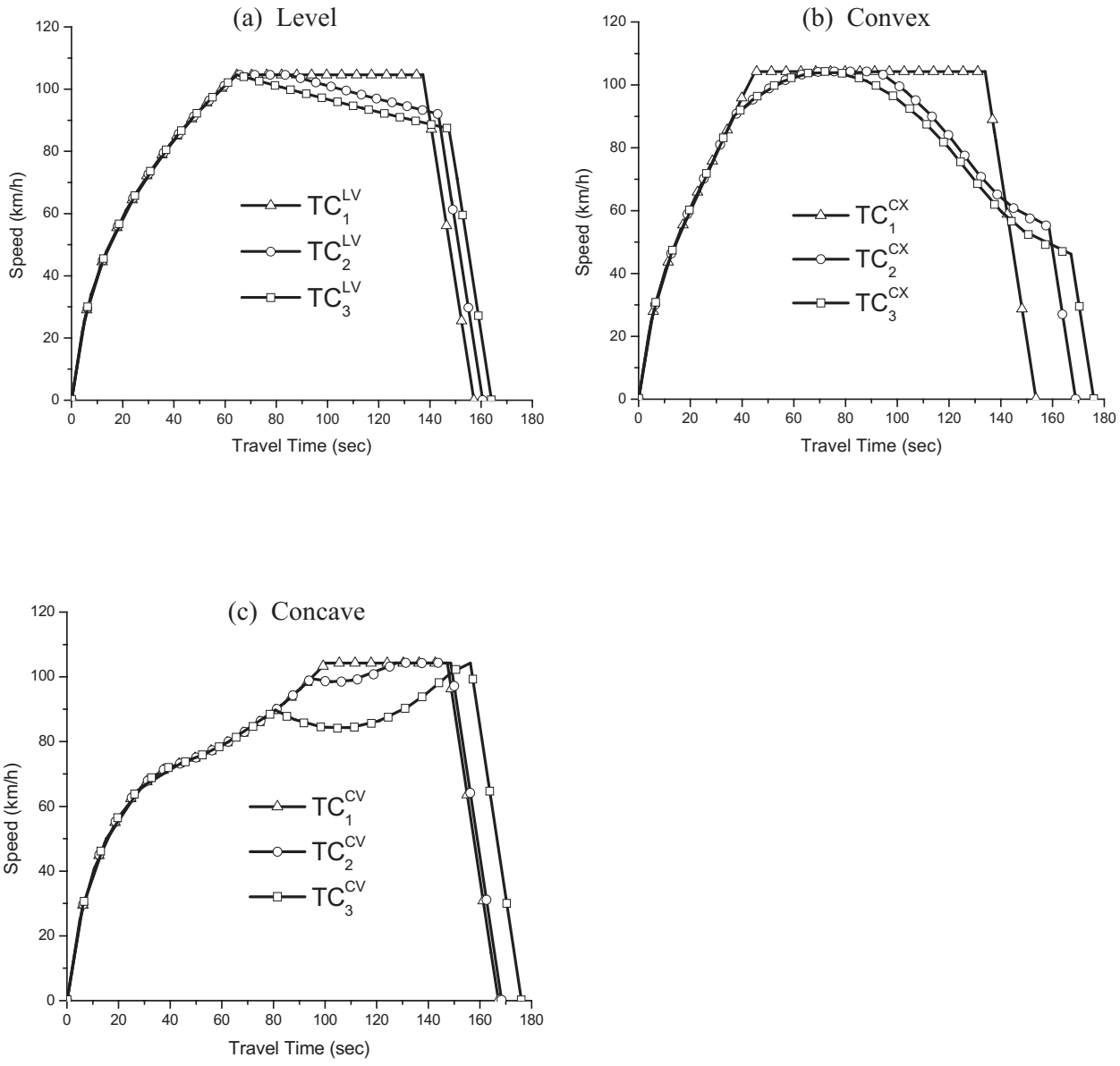

Fig. 7. Speed versus travel time for various train controls

J. Transp. Eng. 2010.136:937-948.

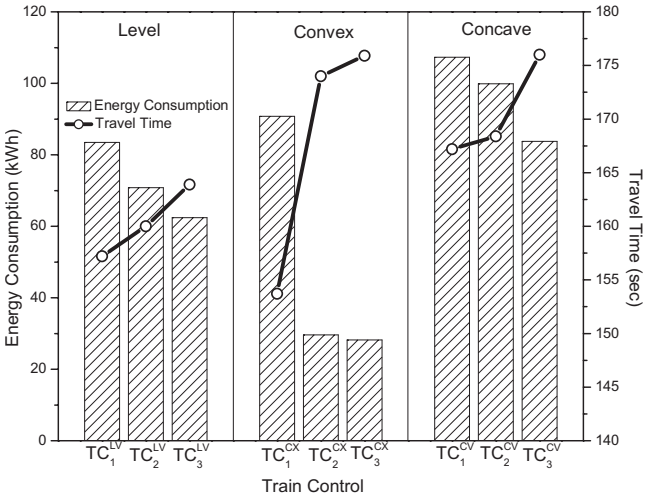

Fig. 8. Energy consumption and travel time

coasting for train controls 2 and 3 on a convex track alignment, denoted as TC_2^{CX} and TC_3^{CX}, respectively, can be successfully performed, which resulted in reduce energy consumption, albeit the travel time increases. For TC_3^{CX}, longer travel time was required because cruising (maximum speed operation) was not applied.

For a concave alignment as shown in Fig. 7(c), the travel time needed for TC_2^{CV} and TC_3^{CV} was affected by the speed that the 1st coasting started. It was found that travel time drastically increases as the 1st coasting started at lower speed. Additionally, longer travel time was taken to reach the maximum operating speed because acceleration is performed for up-hill alignment.

Estimation of Energy Consumption

After having analyzed the variation of travel times for various train controls and track alignments, the resulting energy consumptions and travel times are shown in Fig. 8. It was found that both travel time and energy consumption are sensitive to the geometry of track alignment as well as the train control, denoted as (TC_s^{α}). Note that α represent the index of track alignments [i.e., *L* (LV), convex (CX), and concave (CV)] and *s* represents train control scenarios discussed in TCM. As shown in Fig. 8, the least energy consumption is yielded by applying TC_3^{CX} on a convex alignment with train control associated with acceleration, 1st coasting, cruising, 2nd coasting, and braking regimes, while TC_1^{CV} on a concave alignment consumed the greatest energy to complete a journey. An interesting observation in Fig. 8 was found that the travel time ranges under a level, convex, and concave alignments are 156–162 s, 153–176 s, and 166–176 s, respectively. Operating a train under a convex alignment not only yields the least energy consumption but a greater range of travel time, which provides transit operators more flexibility to justify train control to meet scheduled arrival time at the downstream stop.

Sensitivity Analysis

At the beginning of this section, the effects of the coasting position and travel time constraint on energy consumption and travel time are focused. Figs. 9(a) indicates the effect of the 2nd coasting position on energy consumption and travel time, while the maximum operating speed (V_M) is 105 km/h It was found that the earlier the coasting starts, the less the energy was consumed, yet the travel time increases.

Considering the travel time constraint, Fig. 9(a) can be applied to determine the position where the 2nd coasting should start. For example, if the scheduled travel time is 160 s between a pair of stations with a convex alignment, the distance from the upstream station to the coasting position must be greater than 2,603 m as shown in Fig. 9(b); otherwise, the train will be late at the next station. However, if the track alignment is level, the coasting regime must start at 1,918 m or later from the upstream station to ensure that the travel time is less than 160 s [see Fig. 9(c)]. The consumed energy associated with the 2nd coasting on the convex track alignment was 49.3 kWh, which is significantly less than that on the level track alignment with 68.7 kWh.

Considering various scheduled travel times while fixing the location for the 1st coasting at 525 m from station A, the optimal 2nd coasting positions which minimize the energy consumptions for level and convex track alignments were found numerically. In Fig. 10, as allowable travel time increases (e.g., due to an early arrival of a train at the upstream station), the optimized coasting position is moving toward to the downstream station to further reduce energy consumption. However, if the allowable travel time is fairly long (e.g., greater than 164 and 176 s for level and convex, respectively), the coasting may be triggered before reaching V_M. On the other hand, if the allowable travel time is short (e.g., shorter than the minimum travel time, 157 and 155 s for level and convex alignments, respectively), the coasting regime shouldn't be applied and the maximum energy will be consumed, yet the train arrival delay can be reduced.

Conclusions and Future Research

A TPS model is developed in this study, which provides rail operators a useful tool to simulate train movement, calculate energy consumption, and estimate travel time, considering various vertical track alignments and train controls on a time-driven basis. In addition, the acceleration/deceleration rate, speed, energy consumption rate, and travel distance can be generated according to user specified time interval.

As discussed in the numerical example, the proposed TPS model has demonstrated itself a potential approach to explore and quantify the benefit of optimal train control on various track alignments with speed and travel time constraints. The results of the numerical example indicated that appropriately performing the coasting regime might save up to 66.7% reduction of energy consumption (when coasting begins at the optimal location on a convex-up alignment) yet the travel time increased. It is worth noting that the level of energy saving is depending on the track alignment, the timing and location as the coasting regime is triggered, maximum operating speed, and allowable travel time.

In order to provide the desired level of confidence in the result generated by the developed TPS, train performance parameters such as transmission efficiency (η), acceleration/deceleration rates, and braking efficiency need to be calibrated. Especially, the value of η can be acquired by tractive effort and train speed, which significantly affects total energy consumption.

The immediate extension of this study is to enhance the developed TPS by considering more realistic track alignment, including the combination of level, convex and concave alignments in a rail line segment with variable maximum operating speed require-

J. Transp. Eng. 2010.136:937-948.

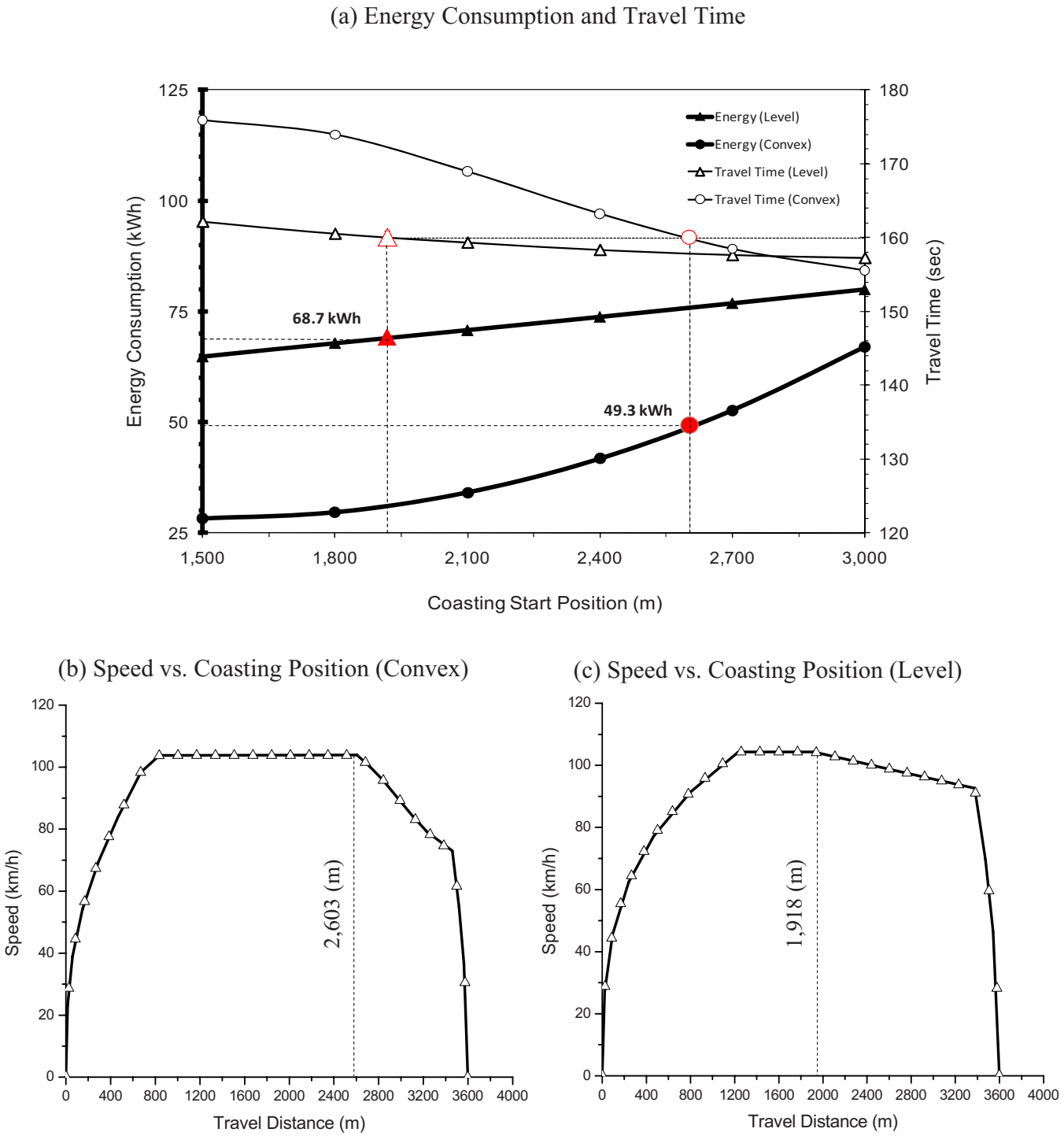

Fig. 9. Energy consumption and travel time versus the coasting position (V_M=105 km/h)

ments. Note that the coefficient of adhesion discussed in Eq. (3) and bearing and rolling resistance discussed in Eq. (5) were found nonlinear with an increasing speed in previous studies (Candee 1940; Bernsteen et al. 1983), which can be adapted by the developed TPS for better estimation of energy consumption. Additionally, the joint effect of the horizontal and the vertical track alignments considering regenerative braking system on energy consumption and travel time may be considered while enhancing the TPS developed in this study.

Notation

The following symbols are used in this paper:

a_{max} = maximum acceleration rate (ft/s^2);
a^t = acceleration rate at time t (ft/s^2);
$\bar{a}$ = average speed change rate of acceleration (ft/s^2);
b_{max} = maximum deceleration rate (ft/s^2);
b^t = deceleration rate at time t (ft/s^2);

J. Transp. Eng. 2010.136:937-948.

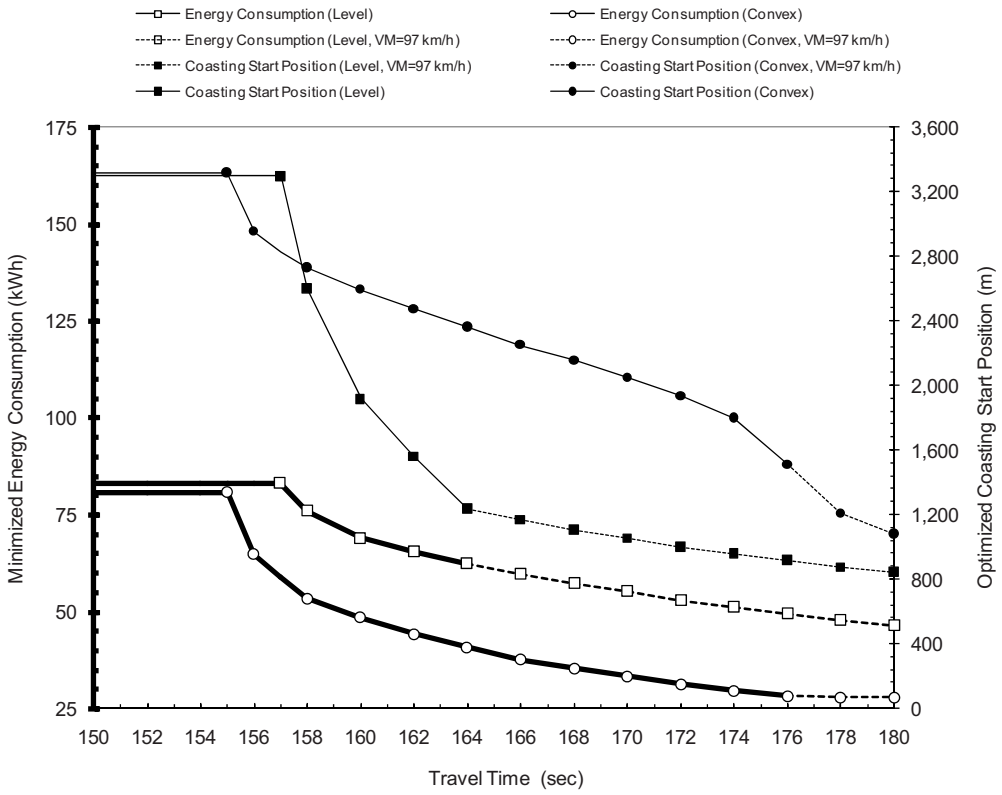

Fig. 10. Coasting position and energy consumption versus allowable travel time

$\bar{b}$ = average speed change rate of deceleration (ft/s^2);
$\overline{c_1}$ = average speed change rate of deceleration (ft/s^2);
$\overline{c_2}$ = average speed change rate of 1st coasting (ft/s^2);
D^t = track curvature at time t (degrees);
d = maximum depth/height at middle of station spacing (ft);
E = total energy consumption (kWh);
e^t = energy consumption rate at time t (kWh);
F_a^t = adhesive force at time t (lb);
$F_{B(\max)}^t$ = maximum braking force (lb);
F_{ba}^t = adhesion-limited braking force (lb/train);
F_{bc}^t = comfort-limited braking force (lb/train);
$F_{\max}^t$ = maximum tractive effort at time t (lb);
F_p^t = propulsive force at time t (lb);
F_{TE}^t = applied tractive effort at time t (lb);
G_i^t = track grade where x^t traveled at time t on segment I (%);
g = gravitational acceleration (ft/s^2);
I_i = track Alignment inflection point at ith segment;
J = number of time steps required for traveling;
L_i = horizontal track length at ith segment (ft);
l = track length required for vertical curves (ft);
M_a = acceleration regime;
M_b = braking regime;
M_{c_1} = 1st coasting regime;
M_{c_2} = 2nd coasting regime;
M_v = cruising regime;
m = train mass (lb);
N_{TR} = number of cars per train;
n = number of axles per car;
P^t = engine horse power at time t (hp);
q = number of vertical segments determined by inflection points;
R_T^t = total train resistance at time t (lb);
R_U^t = unit resistance per axle at time t (lb/t);
S = station spacing (ft);
S_a = travel distance during accelerating (ft);
S_b = travel distance during braking (ft);
S_{c_1} = travel distance during 1st coasting (ft);
S_{c_2} = travel distance during 2nd coasting (ft);
S_v = travel distance during cruising (ft);
s = index of train control scenarios;
T = total travel time (s);
t_a = acceleration time (s);
t_b = braking time (s);
t_{c_1} = 1st coasting time (s);
t_{c_2} = 2nd coasting time (s);
t_v = cruising time (s);
V_M = maximum operating speed (mi/h);
V_b = critical speed (mi/h);
V_{c_1} = speed at 1st coasting starts (mi/h);
V^t = train speed at time t (mi/h);
V_{wd}^t = wind speed at time t (mi/h);
W = train weight (lb);
x^t = traveled distance at time t (ft);
y_i^t = vertical track alignment where x^t traveled at time t on segment i (ft);
α = index of track alignment;
γ = track transition rate in grade in 100 ft;
δ_1, δ_2 = slope of the two adjacent grades;

J. Transp. Eng. 2010.136:937-948.

η = transmission efficiency;
θ^t = track angle to the horizontal (degree);
θ^t_{wd} = angle between the directions of wind and train movement at time t (degree);
μ^t = adhesion coefficient at time t;
ρ = rotating mass coefficient;
1 ft = 0.3048 m;
1 hp = 0.7457 kW;
1 mi/h = 1.609 km/h;
1 lb = 0.448 N; and
1 t = 907.18 kg.

References

American Railway Engineering Association (AREA). (1981). *Manual for railway engineering*, AREA, Washington, D.C., 16-2-2–16-2-3.

Bernsteen, S. A., Uher, R. A., and Romualdi, J. P. (1983). "The interpretation of train rolling resistance from fundamental mechanics." *IEEE Trans. Ind. Appl.*, IA-19(5), 802–817.

Candee, A. H. (1940). *Electrical equipment for railroad diesel motive power*, Westinghouse Electric & Manufacturing Company, West Mifflin, Pa.

Chang, C. S., Chua, C. S., Quek, H. B., Xu, X. Y., and Ho, S. L. (1998). "Development of train movement simulator for analysis and optimization of railway signaling systems." *Proc., Int. Conf. on Developments in Mass Transit Systems*, Vol. 453, IEEE, New York, 243–248.

Davis, W. J., Jr. (1926). "Tractive resistance of electric locomotives and cars." *Gen. Electr. Rev.*, 29, 685–708.

Energy Information Administration (EIA). (2007). "Average revenue per kilowatt-hour from retail sales to ultimate consumers—Estimated by sector, by state." ⟨http://www.eia.doe.gov/cneaf/electricity/epm/table5_6_a.html⟩ (August 17, 2008).

Gordon, S. P., and Lehrer, D. G. (1998). "Coordinated train control and energy management control strategies." *Proc., 1998 ASME/IEEE Joint*, IEEE, New York, 165–176.

Hay, W. W. (1982). *Railroad engineering*, 2nd Ed., Wiley, New York.

Hoberock, L. L. (1977). "A survey of longitudinal acceleration comfort studies in ground transportation vehicles." *ASME J. Dyn. Syst., Meas., Control*, 99(2), 76–84.

Hopkins, J. B. (1975). "Railroads and the environment-estimation of fuel consumption in rail transportation volume I: Analytical model." *Rep. No. PB-244150*, Federal Railroad Administration, Springfield, Va.

Hopkins, J. B., Hazel, M. E., and McGrath, T. (1978). "Railroads and the environment-estimation of fuel consumption in rail transportation volume III: Comparison of computer simulations with field measurements." *Final Rep. No. FRA-OR&D-75-74.III to U.S. Federal Railroad Administration and Rep. No. PB-288866*, National Technical Information Service, Springfield, Va.

Howard, S. M., Linda, C. G., and Wong, P. J. (1983). "Review and assessment of train performance simulation models." *Transp. Res. Rec.*, 917, 1–6.

Jong, J. C., and Chang, S. (2005a). "Algorithms for generating train speed profiles." *J. East. Asia Soc. Transp. Stud.*, 6, 356–371.

Jong, J. C., and Chang, S. (2005b). "Models for estimating energy consumption of electric trains." *J. East. Asia Soc. Transp. Stud.*, 6, 278–291.

Julich, P. M., Martin, C. G., Brazelton, S. L., and Curtiss, D. F. (1999). "Evaluating the potential benefits of a rail traffic movement planning algorithm." *Proc., 1999 Winter simulation Conf.*, ACM, New York, 1181–1185.

Kim, D. N., and Schonfeld, P. M. (1997). "Benefits of dipped vertical alignments for rail transit routes." *J. Transp. Eng.*, 123, 20–27.

Minciardi, R., Savio, S., and Sciutto, G. (1994). "Models and tools for simulation and analysis of metrorail transit systems." *Computers in Railways IV*, 1, 391–402.

Smith, M. E., Patel, P. K., Resor, R. R., and Kondapalli, S. (1990). "Benefits of the MEET/PASS planning and energy management subsystems of the advanced railroad electronics systems (ARES)." *Transportation Research Forum*, 30(2), 301–309.

Uher, R. A., and Disk, D. R. (1987). "A train operations computer model." *Computers in railway operations*, T. K. S. Nurthy et al., Computational Mechanics Publications, Southampton, U.K., Boston.

Vuchic, V. R. (2007). *Urban transit system and technology*, Wiley, New York.

Yasukawa, S., Fujita, S., Hasebe, T., and Sato, K. (1987). "Development of an on-board energy saving train operation system for the shinkansen electric railcars." *Quarterly Report of Railway Technical Research Institute*, 28, 2–4.

J. Transp. Eng. 2010.136:937-948.